Transient β-Hairpin Formation in α-Synuclein Monomer Revealed by Coarse-grained Molecular Dynamics Simulation

Hang Yu,[1, 2, a)] Wei Han,[1, 3, b)] Wen Ma,[1, 2] and Klaus Schulten[1, 2, 3, c)]
[1)] *Beckman Institute for Advanced Science and Technology, University of Illinois at Urbana-Champaign, Urbana, Illinois 61801, United States*
[2)] *Center for Biophysics and Computational Biology, University of Illinois at Urbana-Champaign, Urbana, Illinois 61801, United States*
[3)] *Department of Physics, University of Illinois at Urbana-Champaign, Urbana, Illinois 61801, United States*

(Dated: 16 November 2015)

[a)] Contributed equally to this work
[b)] Contributed equally to this work; Current address: School of Chemical Biology and Biotechnology, Peking University Shenzhen Graduate School, Shenzhen, Guangdong, 518055, China
[c)] Author to whom correspondence should be addressed. Electronic mail: kschulte@ks.uiuc.edu

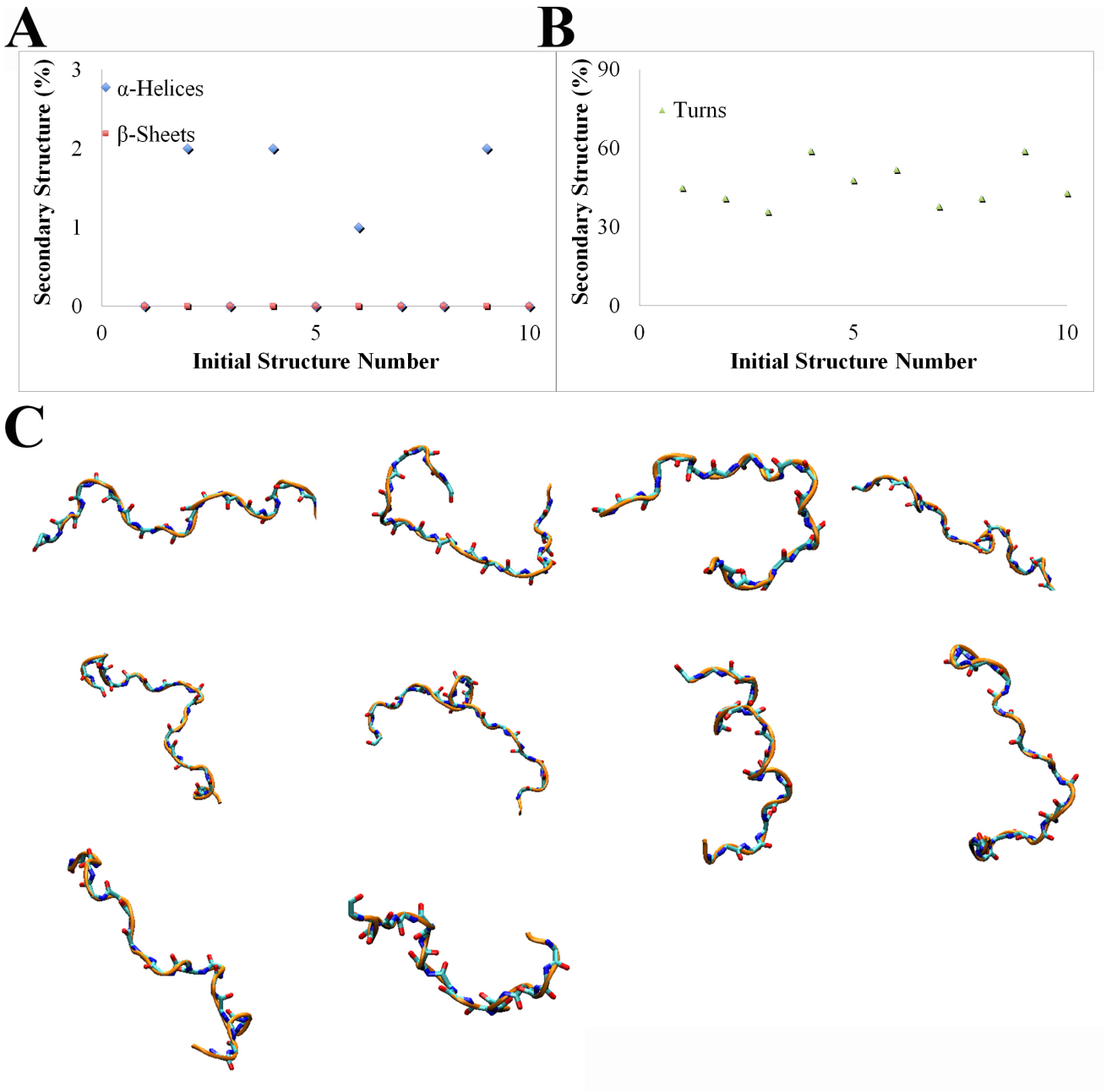

FIG. 1. Secondary structure content and conformations of initial structures. A, B. Secondary structure content in starting structures for α-synuclein simulations (TABLE I). Percentage of α-helix, β-sheet (A) and turn (B) for 10 starting structures of WT α-synuclein simulations are shown in blue diamonds, red squares and green triangles, respectively. Secondary structure contents were analyzed using VMD[1]. C. Conformations of the ten initial structures employed for simulations in the present study. Shown are the backbone atoms of the β-hairpin region (region 38-53) in cartoon (gold) and licorice representations (carbon atoms in light blue, nitrogen in dark blue, oxygen in red and hydrogen in white).

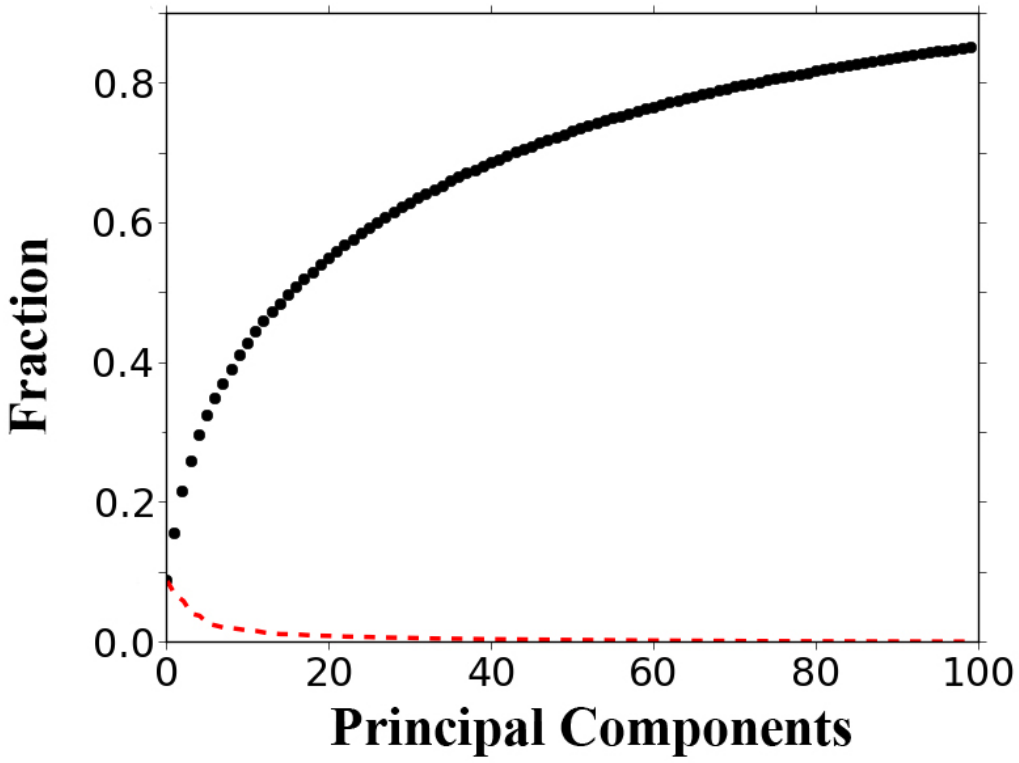

FIG. 2. Individual and accumulated contribution of the first hundred principal components from PCA analysis of simulated WT α-synuclein. Plotted in red dashed line and black dots are the individual and accumulated contributions of structural variation, respectively, of each principal component.

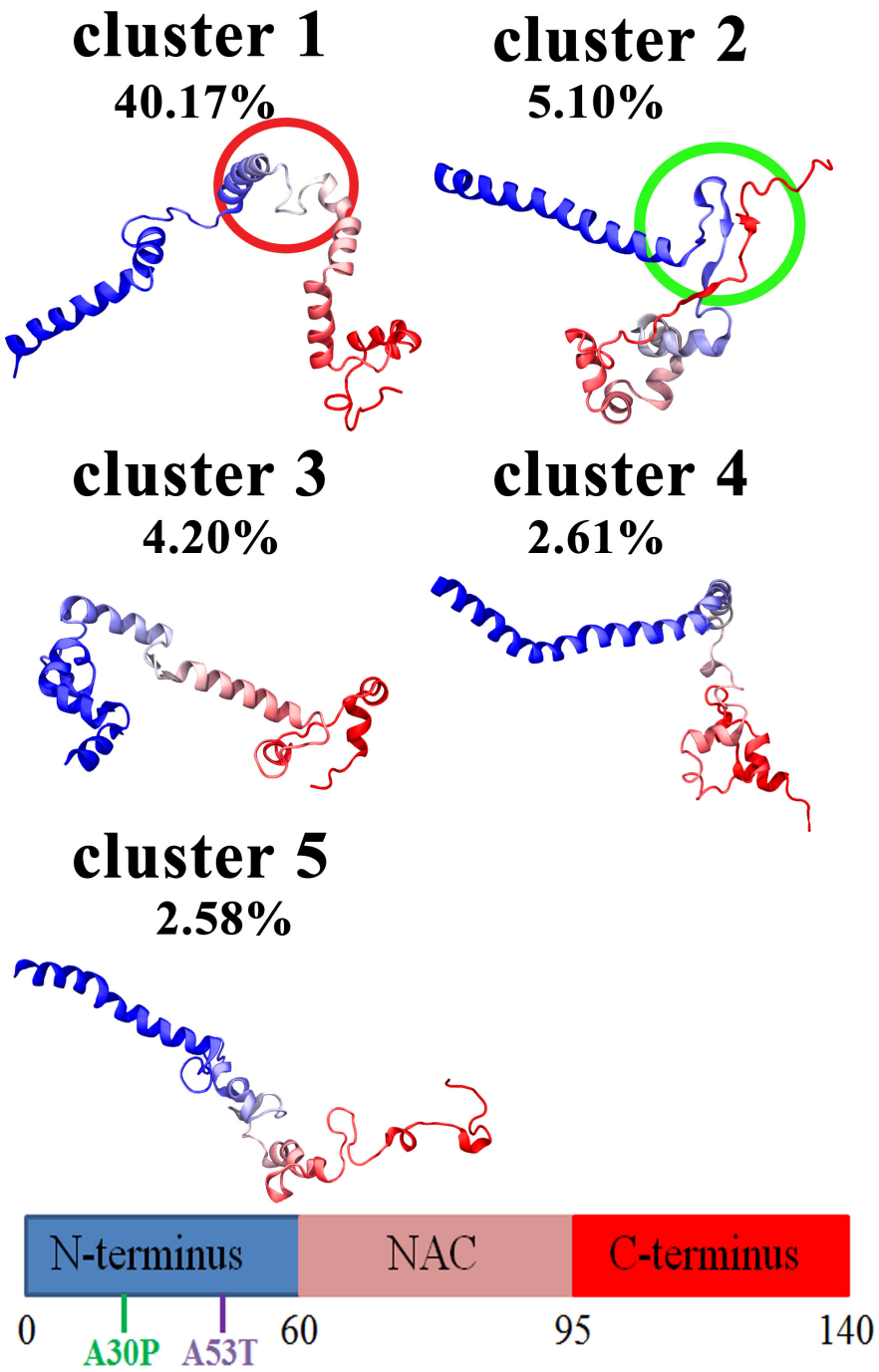

FIG. 3. Representative structures of the five most populated conformational clusters for WT α-synuclein. N-terminus, NAC region and C-terminus are colored blue, pink and red, respectively. The same coloring scheme is applied to further figures of this study. Cluster 2, representing 5.10 % of all conformations, exhibits the formed β-hairpin (see green circle); however, the largest cluster, cluster 1, also exhibits a β-hairpin motif (red circle), but one not yet formed well.

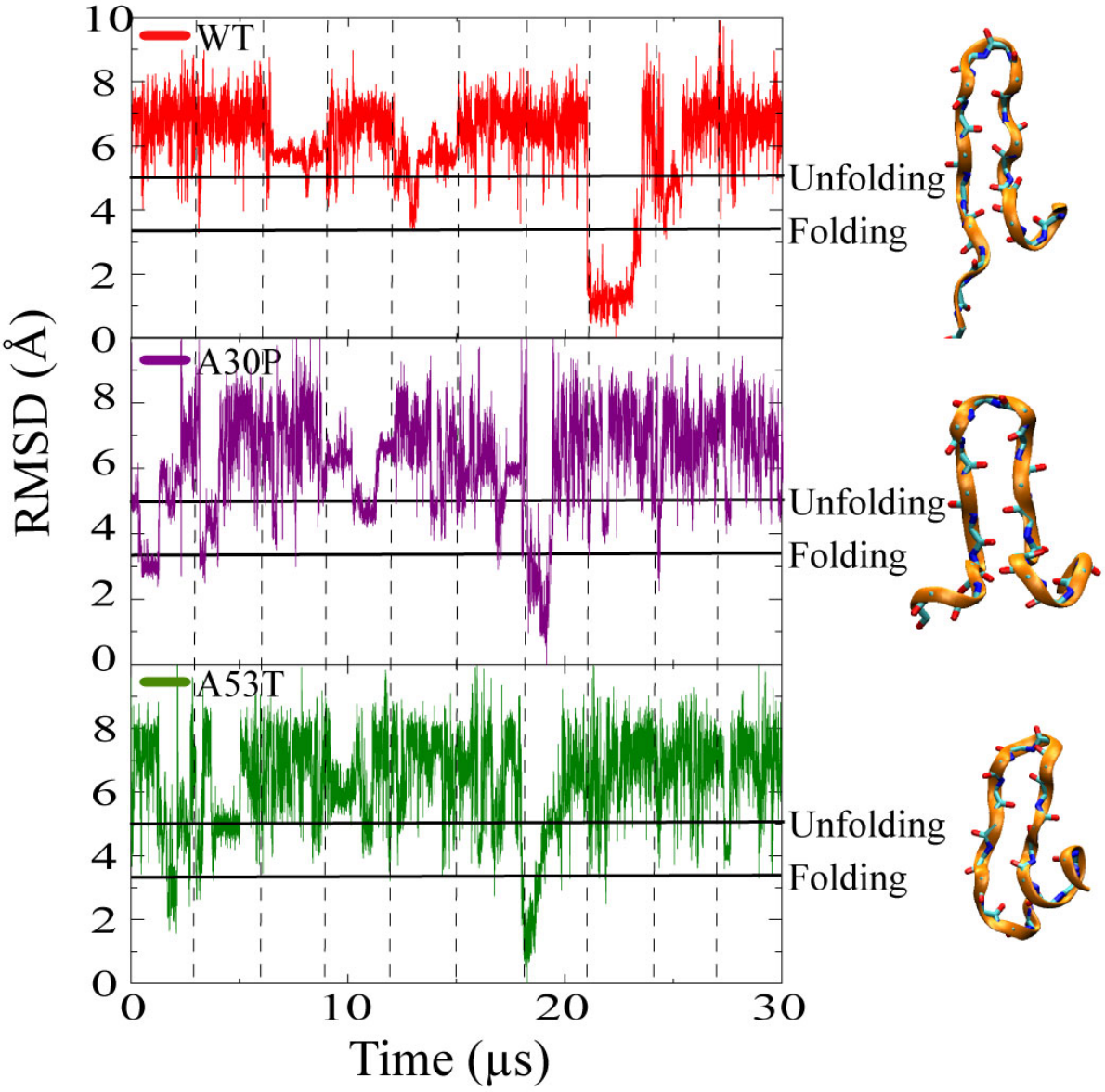

FIG. 4. Hairpin RMSD and representative structures of WT α-synuclein and its A30P, A53T mutants. Plotted are the RMSD values of the β-hairpin region (region 38-53) of WT α-synuclein and its A30P, A53T mutants (in red, purple and green, respectively) over simulation time. Representative structures of the WT α-synuclein and its A30P, A53T mutants are shown on the right. The center structure from the largest cluster of the WT α-synuclein β-hairpin region (region 38-53) was selected as a representative structure for WT α-synuclein. Representative structures of A30P, A53T mutant α-synuclein were obtained with the same procedure in the case of mutant simulations. Backbone atoms of the β-hairpin region (region 38-53) were selected as reference atoms for alignment and RMSD calculation. Individual simulations are separated by dotted lines. The cutoffs defining folding (3.25 Å) and unfolding (5.00 Å) are shown as black lines. A β-hairpin folding event is defined as a transition of the β-hairpin region (region 38-53) from an unfolded state (RMSD $>$ 5.00 Å) to a folded state (RMSD $<$ 3.25 Å).

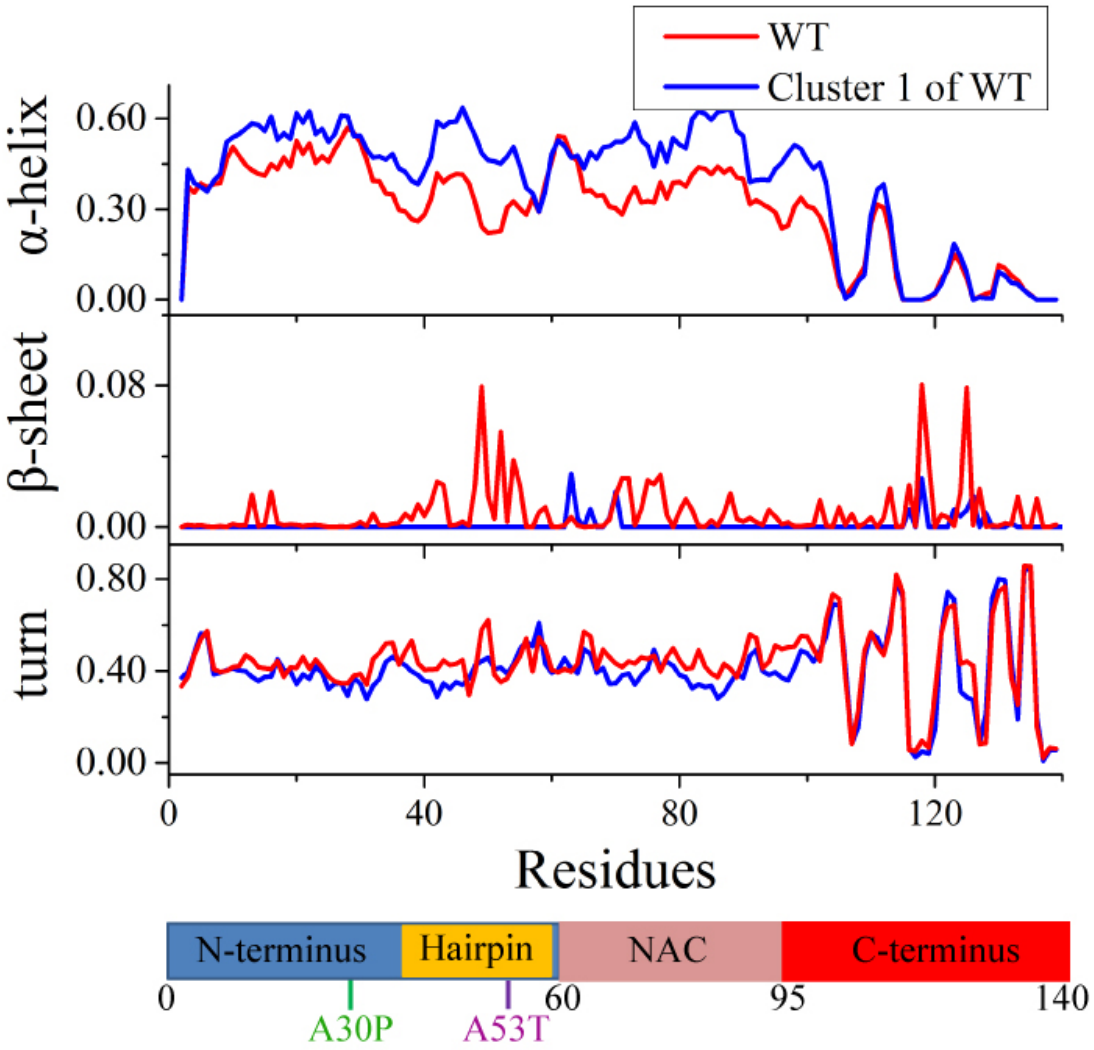

FIG. 5. Residual secondary structure content in WT α-synuclein and its largest cluster, cluster 1. Fractions of α-helix, β-sheet and turn are shown in the top, middle and bottom panels, respectively. The traces for WT α-synuclein and its cluster 1 are colored red and blue, respectively. The x-axis giving residue numbers is also shown as a chain of blue, gold, pink and red bars as defined in FIG. 1.

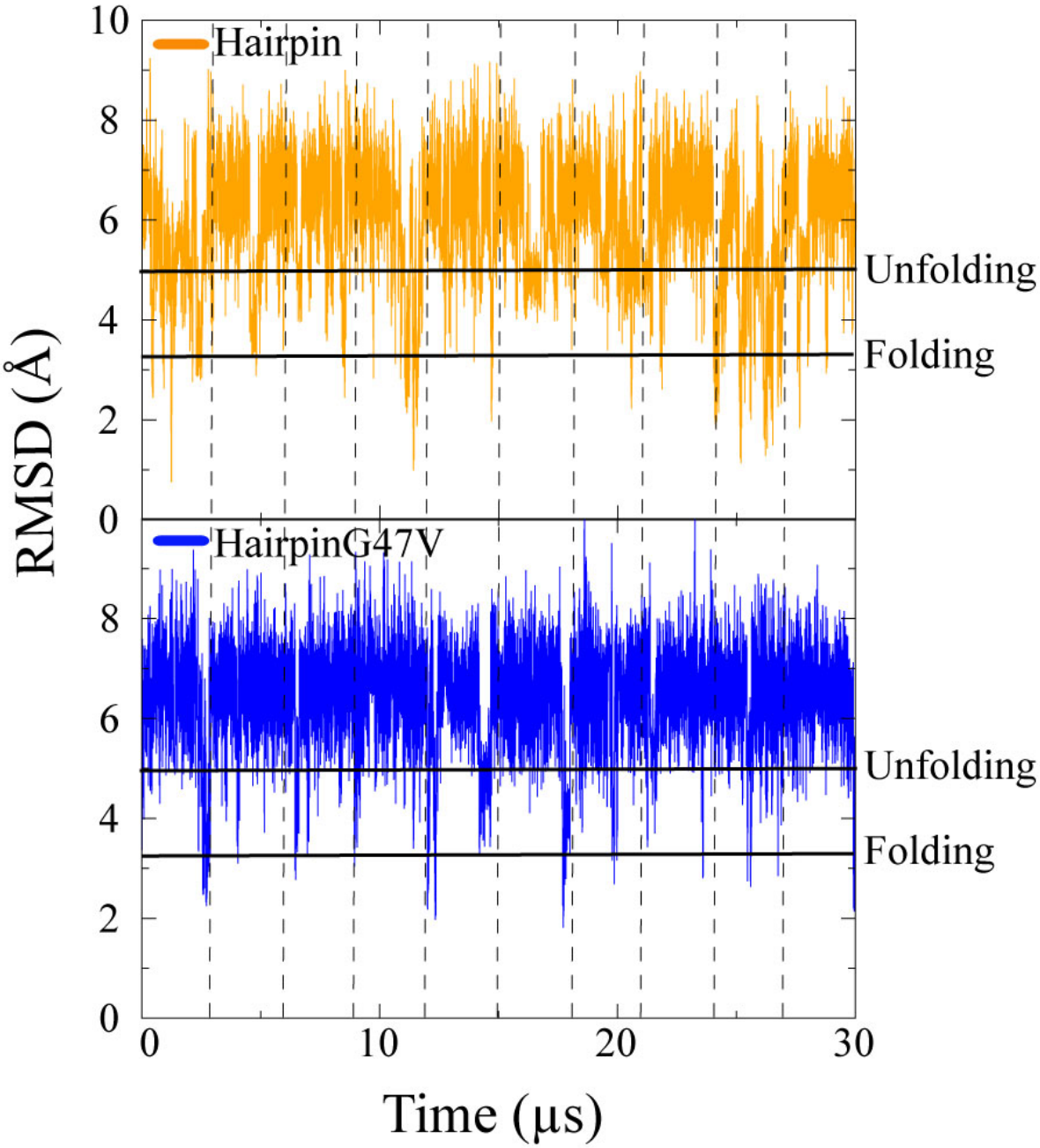

FIG. 6. Hairpin RMSD values arising in simulations of the isolated β-hairpin region (region 38-53) for WT α-synuclein and its G47V mutant. The RMSD values are plotted over simulation time in gold (WT) and blue (G47V), respectively. Backbone atoms of the β-hairpin region (region 38-53) were selected as reference atoms for alignment and RMSD calculation. Individual simulations are separated by dotted lines. The cutoffs defining folding (3.25 Å) and unfolding (5.00 Å) are shown as black lines. A β-hairpin folding event is defined as a transition of the β-hairpin region (region 38-53) from an unfolded state (RMSD $>$ 5.00 Å) to a folded state (RMSD $<$ 3.25 Å).

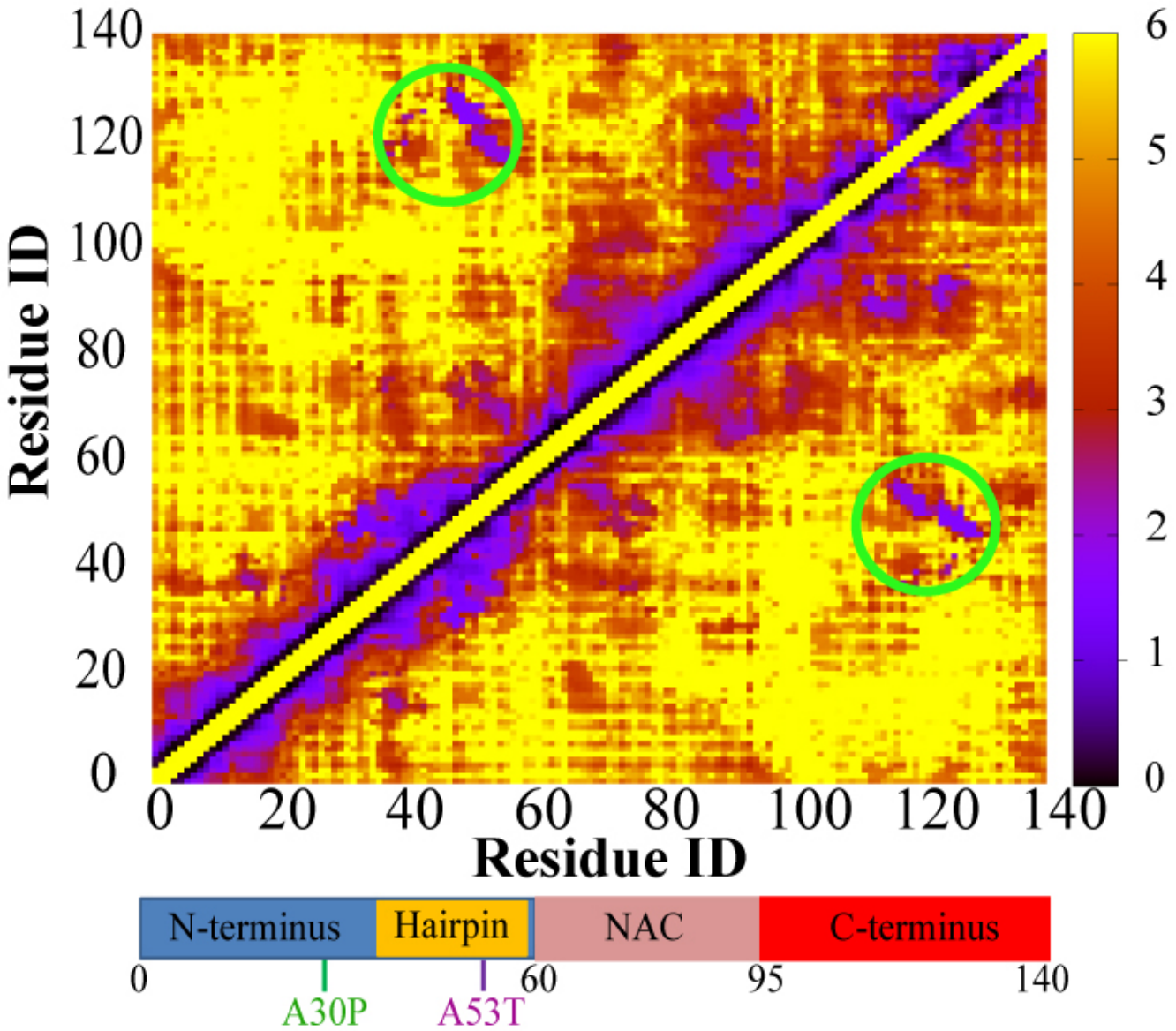

FIG. 7. Contact map of WT α-synuclein. Contacts between β-hairpin structure (region 38-53) and C-terminus (region 118-130) are circled in green (see also FIG. 3, green circle). The probability of contact between residues i and j within the α-synuclein monomer was calculated as the probability for the centers of mass of the two residues to be within a distance of 8.5 Å. Free energy (G) is calculated from residual contact probabilities (P) as G = -$k_BT\times\ln(P)$. Plotted are the contact probabilities from most favorable contact to least favorable contact in terms of relative free energy (kcal/mol). Colors are defined here, as seen in the color bar on the right, in terms of relative free energy (kcal/mol) colored from dark blue to yellow. The x-axis of the contact map is shown as a chain of blue, gold, pink and red bars denoting the positions of N-terminus, β-hairpin region, NAC region and C-terminus on the map, respectively, as defined in FIG. 1. Contacts between adjacent residues are removed for clarity.

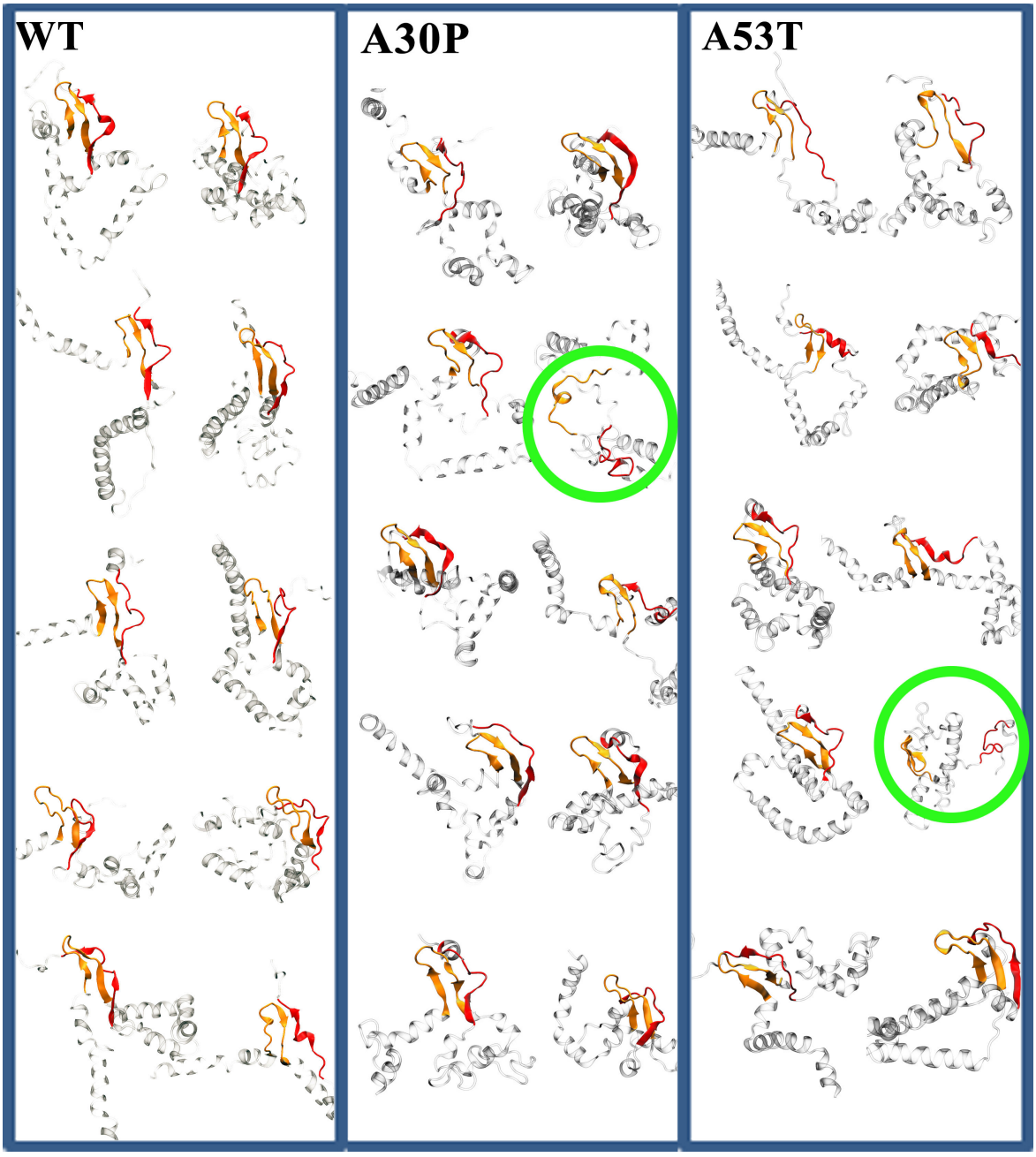

FIG. 8. Stability of interactions between C-terminus and β-hairpin structure in WT α-synuclein and its A30P and A53T mutants. Starting from the center structure of the conformational ensemble containing the β-hairpins (region 38-53) in contact with the C-terminus (region 118-130, FIG. 1B), ten 200-ns simulations were performed for WT α-synuclein and its A30P and A53T mutants (TABLE II, InteractionWT, InteractionA30P and InteractionA53T). Final frames of the 10 simulations are shown in cartoon representation. β-hairpin and C-terminus are shown in gold and red, respectively; the remainder of α-synuclein is shown in grey. The interactions between β-hairpin structure and C-terminus are maintained in most cases (WT: 10/10, A30P: 9/10, A53T: 9/10). Circled in green are the simulations in which the interactions between β-hairpin structure and C-terminus got lost.

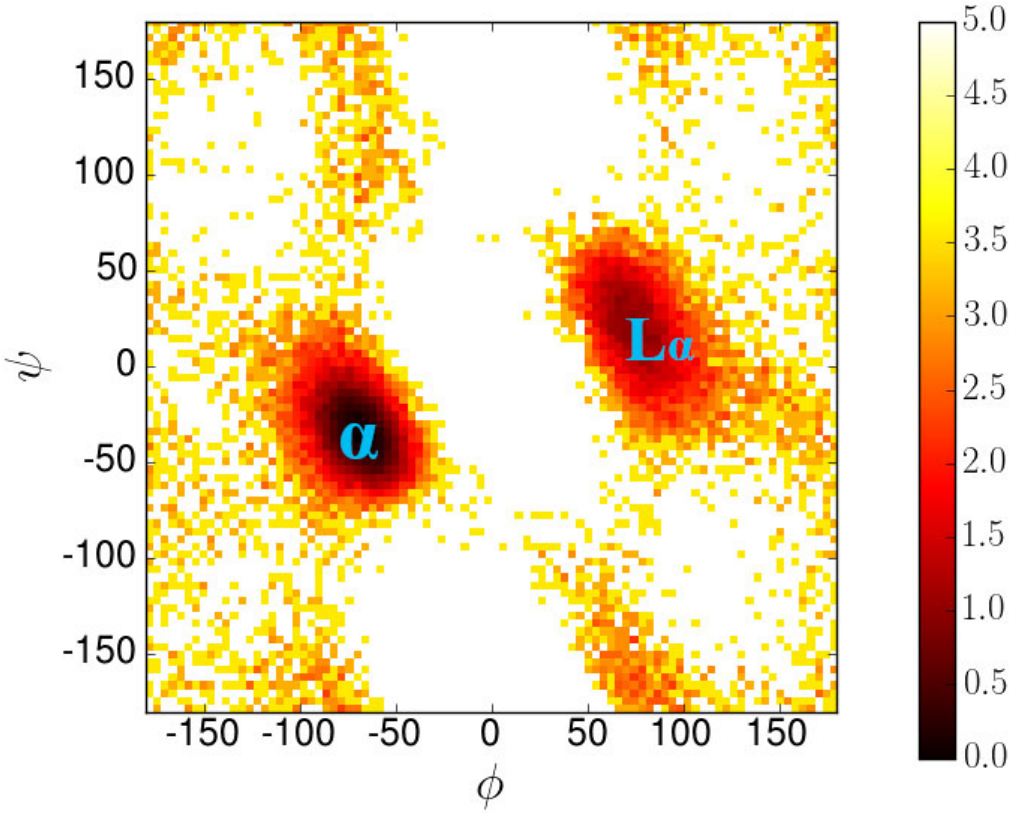

FIG. 9. Ramachandran plot of glycine 47 in the isolated β-hairpin region. This plot illustrates residual structural conformations through backbone dihedral angles ϕ and ψ. Distributions of these angles indicate favorable conformations of glycine 47. Plotted are the dihedral angles ϕ and ψ according to if the angles belong to the most favorable conformation or to the least favorable conformation. Colors are defined here, as seen in the color bar on the right, in terms of relative free energy (kcal/mol) colored from dark red to white. Free energy (G) is calculated from angle distribution probabilities (P) as G = -k_BT×ln(P). Regions on the Ramachandran plot favoring α-helices and left-hand-α-helical conformations are denoted as α and L_α, respectively.

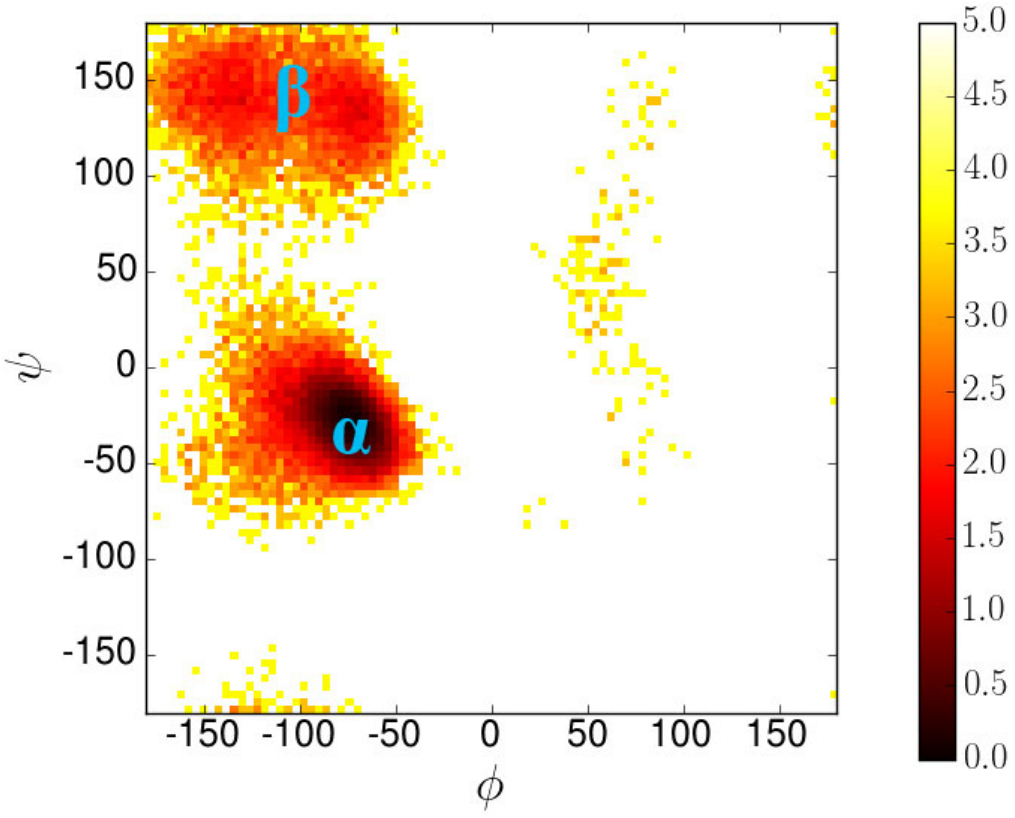

FIG. 10. Ramachandran plot of valine 47 in the isolated β-hairpin region with G47V mutation. This plot illustrates residual structural conformations through backbone dihedral angles ϕ and ψ. Distributions of these angles indicate favorable conformations of valine 47. Plotted are the dihedral angles ϕ and ψ for the valine side group at amino acid sequence position 47. Colors are defined as in FIG. S9. Regions on the Ramachandran plot favoring α-helices and β-sheet conformations are denoted as α and β, respectively.

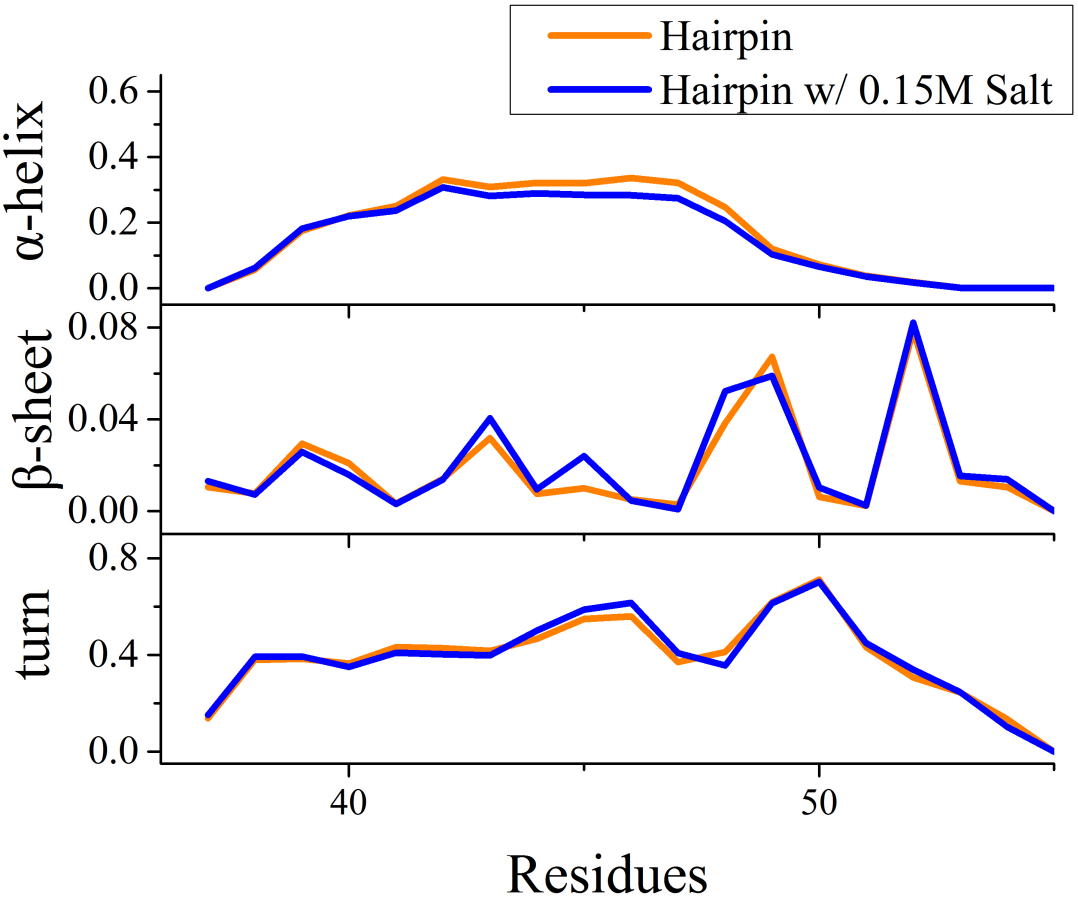

FIG. 11. Residual secondary structure content in isolated β-hairpin region (region 38-53) for WT α-synuclein in water and in the presence of salt. Fractions of α-helix, β-sheet and turn are shown in the top, middle and bottom panels, respectively. The traces for isolated β-hairpin region (region 38-53) for WT α-synuclein in water and in the presence of 0.15M NaCl physiological salt concentration are colored orange and blue, respectively.

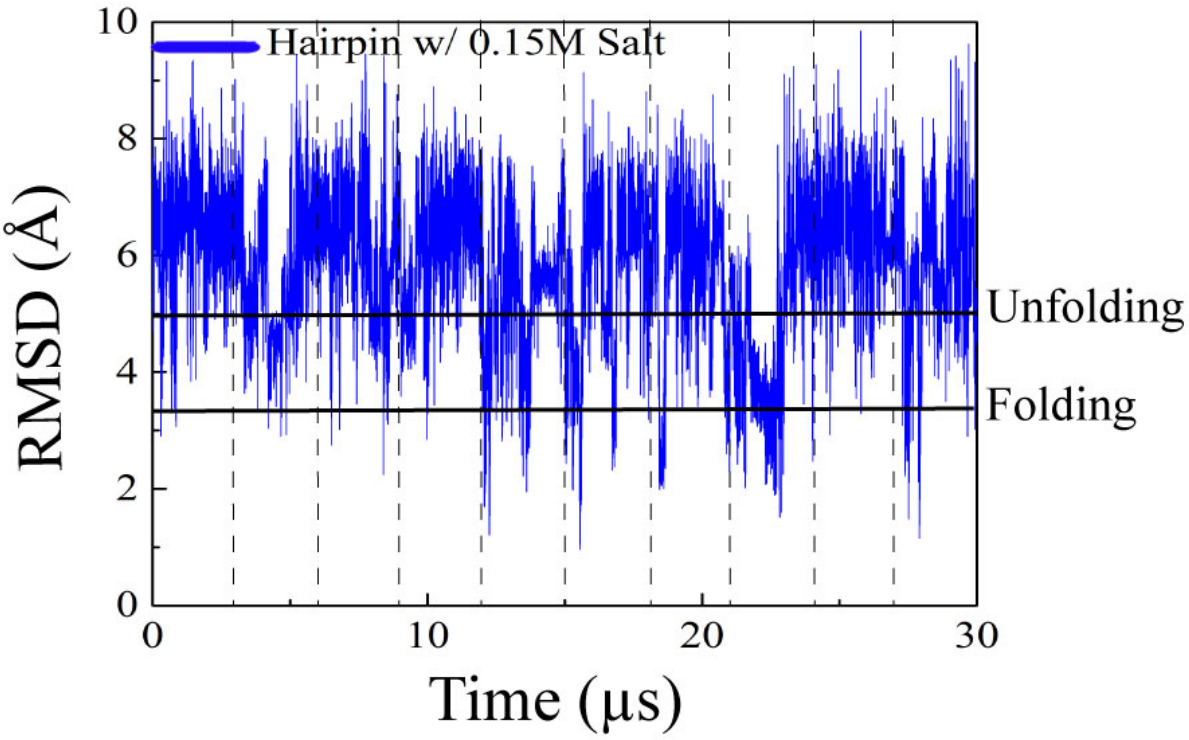

FIG. 12. Hairpin RMSD values arising in simulations of the isolated β-hairpin region (region 38-53) for WT α-synuclein in water and in the presence of salt. The RMSD values are plotted over simulation time in blue (in the presence of 0.15M NaCl physiological salt concentration). Backbone atoms of the β-hairpin region (region 38-53) were selected as reference atoms for alignment and RMSD calculation. Individual simulations are separated by dotted lines. The cutoffs defining folding (3.25 Å) and unfolding (5.00 Å) are shown as black lines. A β-hairpin folding event is defined as a transition of the β-hairpin region (region 38-53) from an unfolded state (RMSD $>$ 5.00 Å) to a folded state (RMSD $<$ 3.25 Å).

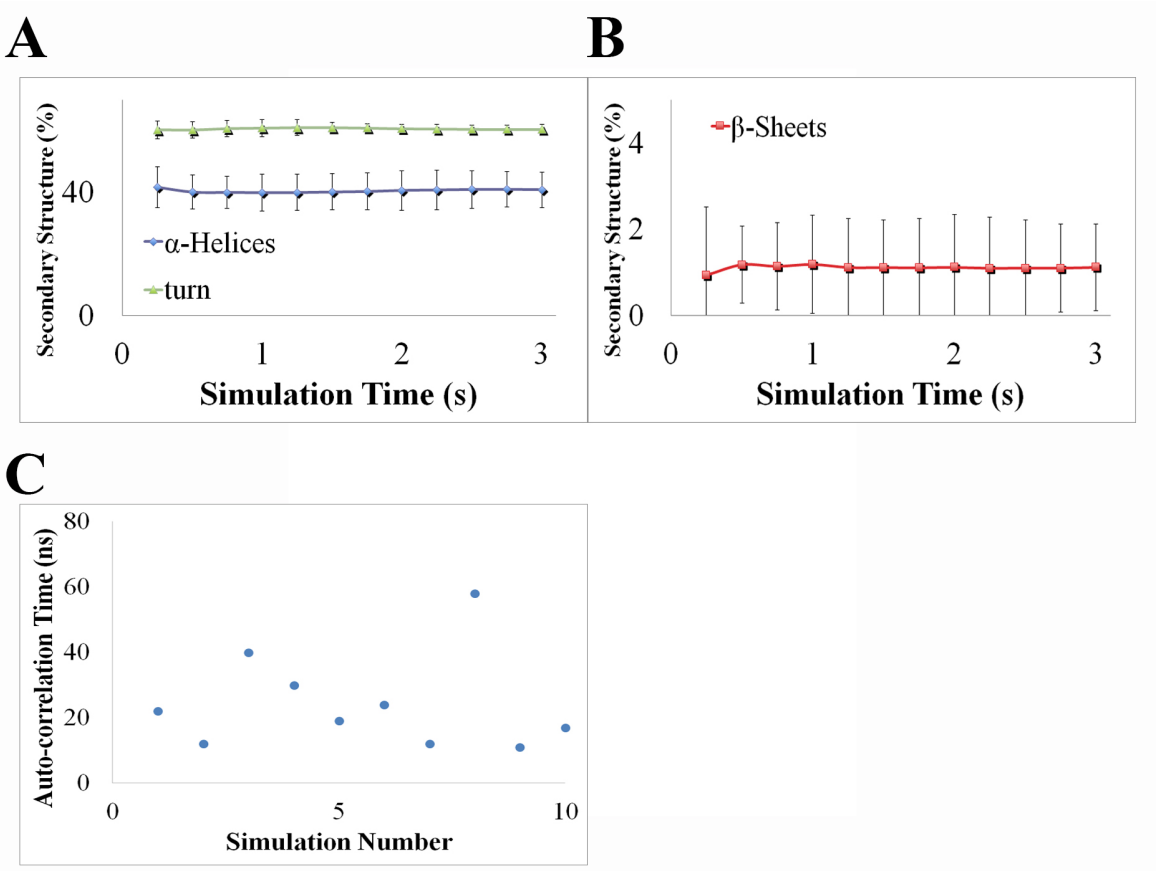

FIG. 13. Secondary structure content and auto-correlation time of end-to-end distance for WT α-synuclein simulations. A, B. Secondary structure content for α-synuclein simulations (TABLE I). Percentage of α-helix, β-sheet (A) and turn (B) averaged over 10 WT α-synuclein simulations are shown in blue diamonds, red squares and green triangles, respectively. Standard deviations are shown in error bars. C. Auto-correlation time of the WT α-synuclein end-to-end distance. For each of the 10 WT α-synuclein simulations, the end-to-end distance was defined as the distance between C_α atoms of residue 1 and 140. The distance was monitored in each simulation over time and fitted into the Python ACOR package[2] to obtain the auto-correlation time.

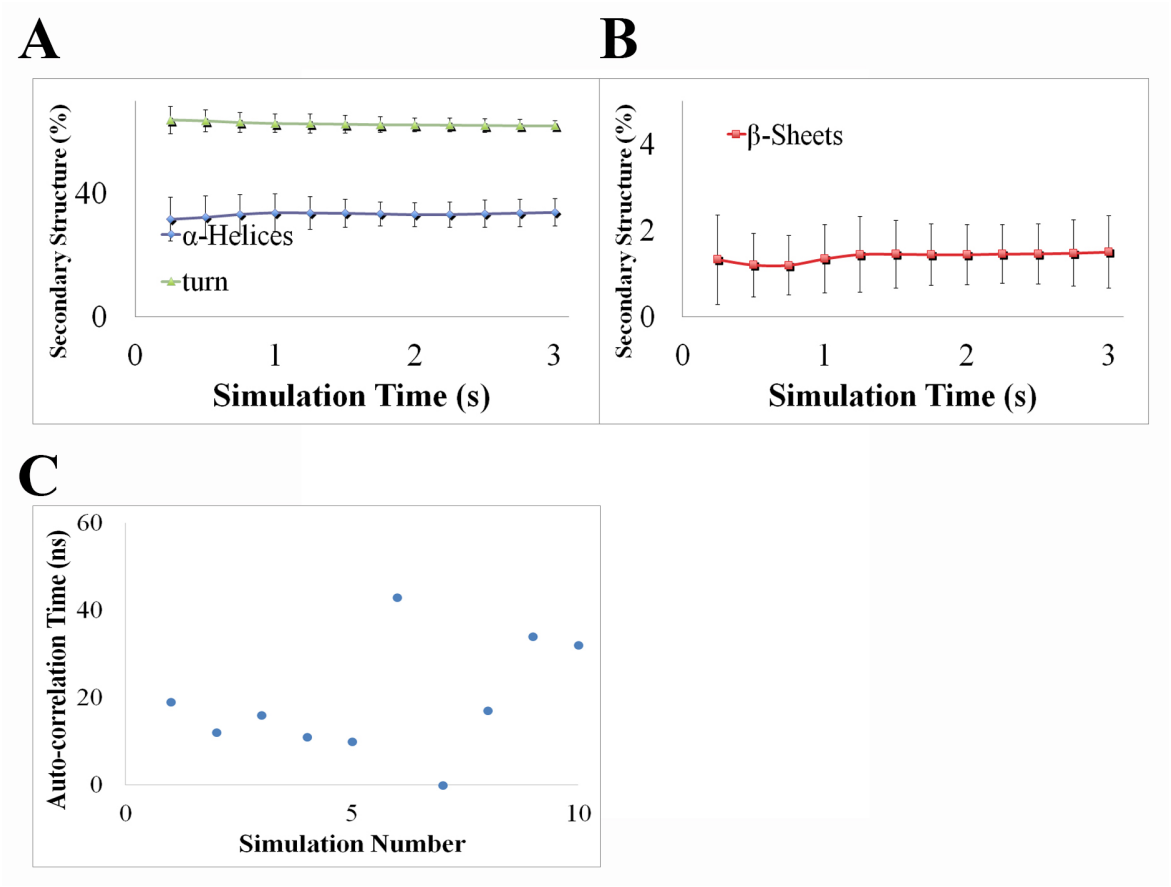

FIG. 14. Secondary structure content and auto-correlation time of end-to-end distance for simulated α-synuclein A30P mutant. A, B. Secondary structure content for α-synuclein A30P mutant (TABLE I). Percentage of α-helix, β-sheet (A) and turn (B) averaged over 10 α-synuclein A30P mutant simulations are shown in blue diamonds, red squares and green triangles, respectively. Standard deviations are shown in error bars. C. Auto-correlation time of the α-synuclein A30P mutant end-to-end distance.

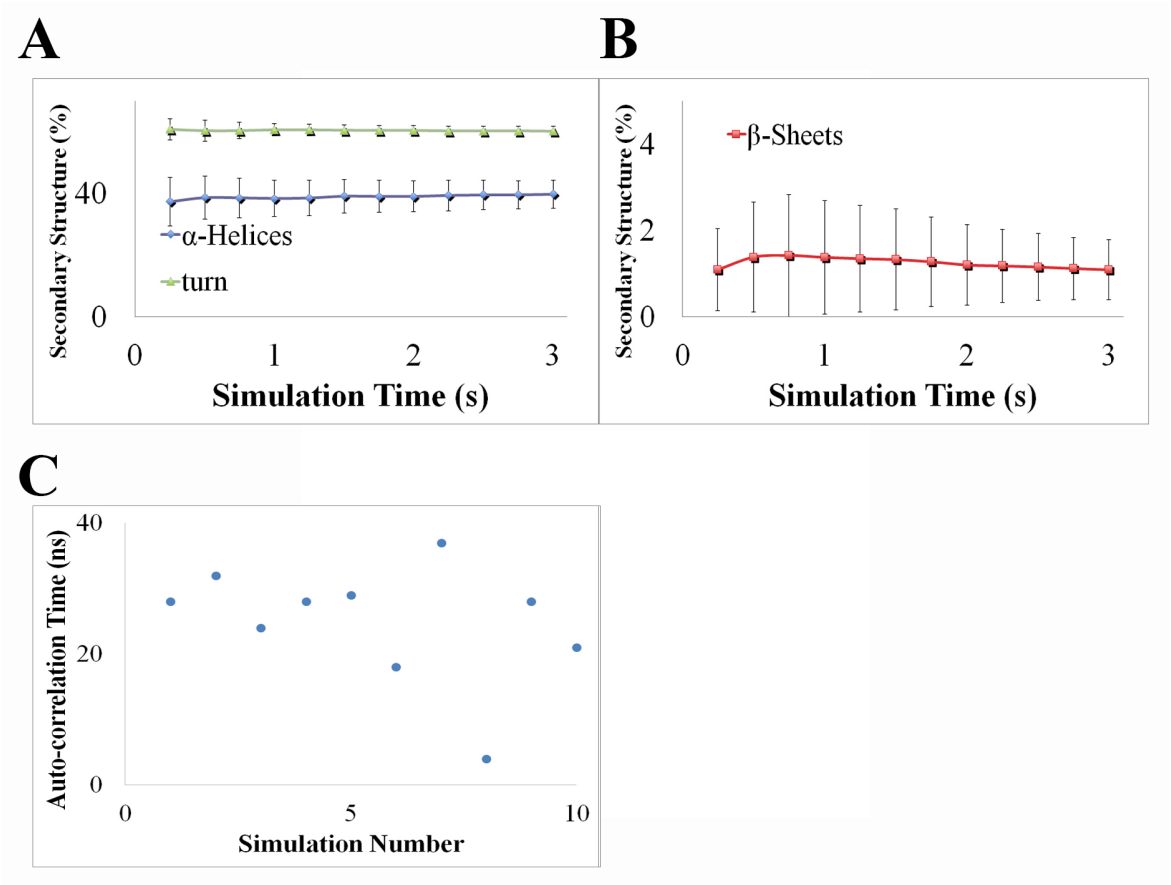

FIG. 15. Secondary structure content and auto-correlation time of end-to-end distance for α-synuclein simulated A53T mutant. A, B. Secondary structure content for α-synuclein A53T mutant (TABLE I). Percentage of α-helix, β-sheet (A) and turn (B) averaged over 10 α-synuclein A53T mutant simulations are shown in blue diamonds, red squares and green triangles, respectively. Standard deviations are shown in error bars. C. Auto-correlation time of the α-synuclein A53T mutant end-to-end distance.

[1]W. Humphrey, A. Dalke, and K. Schulten, "VMD – Visual Molecular Dynamics," J. Mol. Graphics **14**, 33–38 (1996).

[2]A. Sokal, *Monte Carlo methods in statistical mechanics: foundations and new algorithms* (Springer, 1997).